LIST OF TABLES

Page

Table 1. Literature values for original ULR wettability

Reference	ULR	Method used	Original wettability
Odusina, Sondergeld, and Rai (2011)	Eagle Ford Bakken Barnett Floyd Woodford	NMR	Intermediate-wet
Wang et al. (2012)	Middle Bakken Upper Bakken	Amott-Harvey	Oil-wet to intermediate-wet
Shuler et al. (2011)	Middle Bakken	Not reported	Oil-wet to intermediate-wet
Kathel and Mohanty (2013)	Undisclosed	Contact angle	Oil-wet to intermediate-wet
Nguyen et al. (2014)	Eagle Ford	Contact angle	Intermediate-wet
Morsy and Sheng (2014)	Bakken	Contact angle	Intermediate-wet
Mirchi et al. (2014a)	Undisclosed	Contact angle	Water-wet
Mirchi et al. (2014b)	Undisclosed	Contact angle	Intermediate-wet
Alharthy et al. (2015)	Three Folks Bakken	Contact angle	Oil-wet
Habibi et al. (2016)	Montney	Contact angle	Oil-wet and intermediate-wet

From Table 1 most the wettability studies reported oil and intermediate-wet behaviors in ULR. However, some of these studies used different immiscible fluids such as oil and air instead of oil and water, outcrops rather than pay zone samples or performed other wettability measurement methods that may not be suitable for ultralow permeability ULR samples. Nevertheless, further wettability characterization for unconventional resources is needed to have a more comprehensive database. Consequently, this study aims to close that gap in the literature by characterizing the original wettability of Wolfcamp, Bakken, Eagle Ford and Barnett, four of the most important unconventional liquid reservoirs in the United States.

common laboratory setup for imbibition experiments (Cylindrical - All-faces-open), oil recovery can be estimated by a mix of radial and spherical flow.

Table 2. Flow regimes and characteristic lengths for scaling imbibition data.

Boundary Condition	**Flow Regimes**	**Characteristic Length (L_c)**
Open-end-open	Linear	$L_c = l$
Two-ends-open	Radial	$L_c = \frac{d}{2\sqrt{2}}$
Cylindrical (All-faces-open)	Complex	$L_c = \frac{ld}{2\sqrt{d^2 + 2l^2}}$
Sphere	Radial (3D)	$L_c = \frac{d}{2\sqrt{3}}$

Gupta and Civan (1994) and Guo, Schechter, and Baker (1998) worked in addressing the fact that the scaling group proposed by Ma, Morrow, and Zhang (1995) did not consider pore surface wettability; hence, they introduced the effect of wettability in the scaling group as the cosine of the contact angle. This case represented better a wide variety of reservoirs which wettability ranges from oil to water-wet. The dimensionless time was modified as presented in **Eq. 12**.

$$t_D = t\sqrt{\frac{k}{\emptyset}}\frac{\sigma\cos\theta}{\sqrt{\mu_o\mu_w}}\frac{1}{{L_c}^2} \quad \text{..... (12)}$$

experiment results. **Table 3** shows play, well, rock sample depth and reservoir temperature for tested samples.

Table 3. ULR rock sample sources and depths. Reprinted with permission from Alvarez and Schechter (2016c)

ULR	Well	Sample	Depth (ft)	ULR	Well	Sample	Depth (ft)
Bakken **Reservoir Temperature (220 °F)**	Bk-1	1	9620	Barnett **Reservoir Temperature (165 °F)**	Br-1	1	6060
		2	9630			2	8018
		3	9635			3	8582
		4	9640			4	8700
	Bk-2	1	10765		Br-2	1	6896
		2	10770			2	7017
		3	10775			3	7030
		4	10780			4	7616
Eagle Ford **Reservoir Temperature (218 °F)**	EF-1	1	13030	Wolfcamp **Reservoir Temperature (165 °F)**	W-1	1	7790
		2	13040			2	7830
		3	13125			3	7835
		4	13135			4	7880
	EF-2	1	14185			5	7910
		2	14220		W-2	1	8335
		3	14245			2	8370
		4	14250			3	8385
						4	8425

X-ray diffraction and total organic carbon analysis

X-ray diffraction and total organic carbon analysis experiments are conducted to evaluate the nature of the rocks analyzed as well as the lithological variability of ULR with depth. Determine the mineralogical composition of ULR pay zones is critical to select completion fluids that improve water imbibition and favor oil recovering when fracturing the formation (Alvarez and Schechter 2016a). XRD and TOC results for Bakken and Eagle Ford are in **Table 4**.

XRD results for Bakken wells show different lithologies from the two wells analyzed. Well Bk-1 is more siliceous with higher content of quartz whereas well Bk-2

show higher content of dolomite as carbonate dominated. These samples are taken from Middle Bakken (Bk-1) and Three Folks (Bk-2) units showing low TOC values and 25 to 30 wt.% of mainly illite and mica clays. On the other hand, Eagle Ford samples from two wells are more consistent in lithology with all samples tested showing higher carbonate contents at different depths and 20 to 30 wt% of clay content; in addition, TOC values are higher than Bakken, especially in well EF-2. For both reservoirs, illite/smectite content is elevated as an indication of immature clay system.

Table 4. XRD and TOC results for Bakken and Eagle Ford. Reprinted with permission from Alvarez and Schechter (2016c)

Well / Sample	**Bk-1/1**	**Bk-2/1**	**EF-1/1**	**EF-1/2**	**EF-1/3**	**EF-1/4**	**EF-2/1**	**EF-2/2**	**EF-2/3**	**EF-2/4**
Mineral Composition (wt%)										
Quartz	53	14	15	17	13	10	15	15	16	15
Clays	29	26	31	35	33	24	20	19	23	25
Calcite	3	0	46	40	44	59	59	58	54	52
Dolomite	4	51	2	1	1	1	0	2	1	1
Feldspar	9	9	1	3	5	1	1	1	1	2
Pyrite	2	0	5	4	4	5	5	5	5	5
Relative Clay (%)										
Illite/mica	69	60	60	65	59	59	60	59	61	54
Illite/Smectite	13	7	40	35	25	26	30	37	32	33
Kaolinite	4	11	0	0	7	10	3	1	2	4
Chlorite	14	22	0	0	9	5	7	3	5	9
TOC (wt%)	0.7	1.1	3.3	4.0	3.5	3.9	5.6	5.2	5.5	5.4

Rock properties for Wolfcamp and Barnett are represented in **Table 5**. Both Wolfcamp wells have variable mineral composition with depth changing from siliceous to carbonate in different strata. In addition, clay content is below 30 wt% and mostly illite and mica. Moreover, Wolfcamp shows relative high TOC values like Eagle Ford. Finally,

Barnett samples show consistent low clay content and low illite/smectite proportions with mixtures in similar proportions of quartz and calcite/dolomite and lower TOC values than Wolfcamp and Eagle Ford.

Table 5. XRD and TOC results for Wolfcamp and Barnett. Reprinted with permission from Alvarez and Schechter (2016c)

Well / Sample	**W-1/1**	**W-1/2**	**W-1/3**	**W-1/4**	**W-1/5**	**W-2/1**	**W-2/3**	**Br-1/1**	**Br-1/2**	**Br-2/3**
Mineral Composition (wt%)										
Quartz	40	13	46	41	8	20	48	48	43	46
Clays	40	15	13	27	11	28	27	8	22	8
Calcite	2	46	2	13	15	31	13	35	18	38
Dolomite	2	19	22	6	64	14	6	6	7	6
Feldspar	7	4	17	10	1	5	11	2	8	1
Pyrite	9	3	0	3	1	2	3	1	2	1
Relative Clay (%)										
Illite/mica	75	74	70	72	78	69	67	91	90	76
Illite/Smectite	25	26	30	28	22	31	33	0	0	24
Kaolinite	0	0	0	0	0	0	0	11	5	0
Chlorite	0	0	0	0	0	0	0	0	5	0
TOC (wt%)	5.0	3.4	5.5	5.7	3.0	4.7	4.3	1.7	4.7	2.5

Scanning electron microscopy imaging

Selected samples from the four plays are imaged using SEM; results are in **Fig. 11** for Bakken and Eagle Ford and in **Fig. 12** for Wolfcamp and Barnett. For Bakken (Fig. 11, top), the SEM images confirm XRD results showing siltstones at 500X optical zoom and presence of chlorite, mica and illite in a siltstone at 2000X. Moreover, Eagle Ford SEM images (Fig. 11, bottom) show calcareous rocks with siltstones, as XRD results, at 600X and the micritic calcite matrix with small dissolution vugs (squares) and rare foram fossils at 2000X.

are lower because they consider air density related by porosity values. Finally, median pore throat radius from these wells shows nanopore sizes, which are common in these types of reservoirs. This small pore radius makes capillary forces significant dominating fluid displacement in the porous media.

Table 6. Petrophysical properties for Bakken, Eagle Ford, Wolfcamp and Barnett. Reprinted with permission from Alvarez and Schechter (2016c)

Well / Sample	**Bk-1/1**	**Bk-2/1**	**EF-2/1**	**W-1/3**	**W-1/4**	**W-2/3**	**Br-1/1**	**Br-1/2**
Porosity (%)	10.8	6.5	8.6	6.8	6.4	6.2	7.8	6.1
Permeability to air (µD)	23.03	0.41	0.47	0.16	0.25	0.18	1.05	0.75
Grain Density (g/cc)	2.72	2.75	2.52	2.59	2.63	2.73	2.63	2.55
Bulk Density (g/cc)	2.43	2.58	2.31	2.41	2.46	2.56	2.43	2.39
Median pore throat radius (µm)	0.034	0.010	0.007	0.003	0.004	0.005	0.008	0.007

In addition, Swanson air permeability is cross-plotted with porosity values in **Fig. 14**. Wolfcamp wells show the lowest values for permeability and porosity while Bakken display different relationship varying by well. Barnett wells show similar permeability varying porosities at different depths. Regardless the small data set; there is a visible trend of increasing permeability as porosity of the sample increments in Barnett and Bakken samples. Now that ULR rock properties have been identified and differentiated, oil properties are studied next to address rock-fluid interactions.

crude oil properties from wells in Bakken, Eagle Ford, Wolfcamp and Barnett are shown in **Table 7**. Using titration methods, TAN and TBN is determined. Bakken oil has higher acid number but the difference between TAN and TBN is not very marked. On the other hand, Eagle Ford oil is more basic as well as Barnett 1 and 2, and Wolfcamp shows more basicity but with a small difference when compared to TAN. Regarding oil densities, all samples can be ranked as light oils at reservoir temperature.

Table 7. Oil properties for Bakken, Eagle Ford, Wolfcamp and Barnett. Reprinted with permission from Alvarez and Schechter (2016c).

ULR	Bakken	Eagle Ford	Wolfcamp	Barnett 1	Barnett 2
TAN (mg KOH/ g oil)	0.36	0.02	0.09	0.27	0.10
TBN (mg KOH/ g oil)	0.23	0.61	0.12	0.55	0.57
API (°) @ 70 °F	35.08	57.4	31.4	30.9	30.2
API (°) @ Res. Temp	37.30	58.7	32.4	37.5	35.8

IFT measurements

Using the pendant drop method, IFTs between water and crude oil from Bakken, Eagle Ford, Wolfcamp and Barnett are measured at reservoir temperature. As represented in **Fig. 15**, Eagle Ford has the highest IFT among the group; then, Wolfcamp, Barnett and Bakken show similar IFT values. Oil-water IFT is a very important parameter to follow when addressing IOR in unconventional reservoirs. As shown in the Young-Laplace equation (Eq. 1), IFT is directly proportional to capillary pressure and its original value and possible alteration is fundamental in favoring oil recovery by spontaneous imbibition (Alvarez et al. 2014, Alvarez and Schechter 2016a, 2017). IFT can be altered by adding

proper surfactants to completion fluids favoring imbibition. In the next section, we address ULR wettability as the other parameter in the Young-Laplace equation that can modify capillary pressure as well as the relation of oil and rock properties in ULR original wetting state.

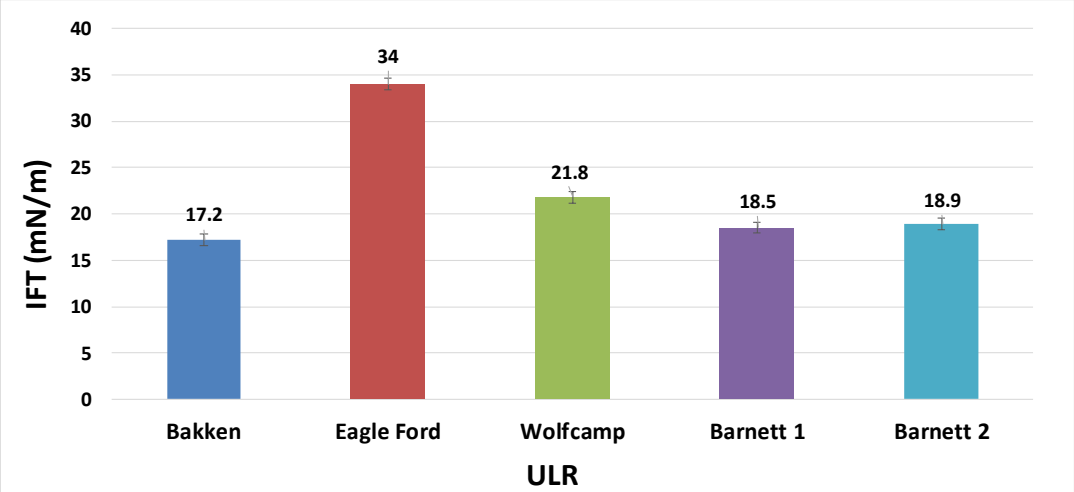

Figure 15. Oil-water IFT for Bakken, Eagle Ford, Wolfcamp and Barnett. Reprinted with permission from Alvarez and Schechter (2016c).

Wettability Measurement Experiments

In this section, I investigate original wettability of different wells from Bakken, Eagle Ford, Wolfcamp and Barnett by contact angle and zeta potential measurements.

Contact angle results

Original rock wettability is measured by CA experiments using the captive bubble method. CA measurements are performed in several samples from different wells in Bakken, Eagle Ford, Wolfcamp and Barnett formations as described in Table 3. To

Spontaneous imbibition of oil into ULR cores

Cores from Bakken, Eagle Ford, Wolfcamp and Barnett are submerged in oil from the same formation inside an environmental chamber to guarantee reservoir temperature. Initial weight and average CT numbers are recorded to address changes at the end of the experiments. After two months, samples are weighted and scanned and the volume imbibed is calculate using oil and water densities. The results are represented in **Table 8.** The main observation from oil imbibition experiments is that all formations let oil spontaneously imbibe into the cores regardless, lithology, petrophysical characteristics and oil type. This confirms the results from previous sections in which CA and zeta potential measurements show intermediate and oil-wet behaviors. When the results are analyzed by ULR, Bakken cores show low percentage of pore volume imbibed with values ranging from 18 to 21%. Imbibition results are consistent with wettability values for Bakken, which have the lowest CA along with Barnett samples. This confirms Bakken intermediate affinity to oil compared to other ULR.

Table 8. Oil spontaneous imbibition experiment results. Reprinted with permission from Alvarez and Schechter (2016c)

ULR	Well / Sample	Penetration magnitude (HU)	Δ Weight (gr)	Volume imbibed (ml)	Pore volume (ml)	% Pore volume imbibed
Bakken	Bk-1/1	49	0.389	0.490	2.697	18.1
	Bk-1/3	52	0.487	0.614	3.520	17.4
	Bk-2/1	51	0.209	0.264	1.277	20.7
	Bk-2/3	44	0.168	0.211	1.231	17.1
Eagle Ford	EF-1/2	95	1.036	1.444	3.155	45.8
	EF-1/4	116	1.041	1.451	3.497	41.5
	EF-2/1	133	1.235	1.721	2.284	75.8
	EF-2/2	139	1.140	1.602	2.567	62.4
Wolfcamp	W-1/3	46	0.599	0.731	1.690	43.3
	W-1/4	48	0.607	0.740	1.625	45.5
	W-2/1	50	0.756	0.922	1.465	62.9
	W-2/3	51	0.787	0.959	1.660	57.8
Barnett	Br-1/1	51	0.080	0.099	0.730	13.6
	Br-2/3	69	0.070	0.087	0.722	12.0

Moreover, Eagle Ford and Wolfcamp cores show higher oil imbibition among the group with values from 41 up to 76% of pore volume imbibed. All samples from these formations are intermediate towards oil-wet as determined in CA experiments and confirmed by spontaneous imbibition. Also, Eagle Ford elevated changes in penetration magnitude is because oil is visible replacing gas and/or air from the cores in much more amount than samples from other ULR. This is clearly observed in **Fig. 21**, and it is attributed to the preservation technique used to store Eagle Ford cores before they were handled to our laboratories.

Spontaneous imbibition of water into ULR cores

Following the same procedure as the previous section, companion cores from the same ULR wells and depths as oil imbibition experiments are submerged in water inside an oven at reservoir temperature for a period of 2 months. After recoding initial and final weight and average CT numbers, water penetration is calculated. The results are shown in **Table 9**. Consistent with wettability results from CA and zeta potential in which all ULR studied present intermediate-wet behavior, water imbibed in all cores analyzed regardless formation, location or lithology. Cores from Bakken, Eagle Ford, Wolfcamp and Barnett not only let oil imbibe but also water into their pores by capillary forces confirming intermediate wetting affinity. When analyzing the results by unconventional formation, Bakken cores suggest higher imbibition by water than oil with percentage of water imbibed of 62 to 66% of the pore volume in contrast to almost 21% by oil. These findings are persistent with CA measurements where wettability is intermediate towards water-wet and invariable for all cores from the two wells.

Table 9. Water spontaneous imbibition experiment results. Reprinted with permission from Alvarez and Schechter (2016c)

ULR	Well / Sample	Penetration magnitude (HU)	Δ Weight (gr)	Volume imbibed (ml)	Pore volume (ml)	% Pore volume imbibed
Bakken	Bk-1/1	66	1.888	1.888	2.897	65.2
	Bk-1/3	55	1.685	1.685	2.697	62.5
	Bk-2/1	26	0.714	0.714	1.231	57.9
	Bk-2/3	30	0.756	0.756	1.181	63.9
Eagle Ford	EF-1/2	52	0.6708	0.671	3.491	19.2
	EF-1/4	43	0.3645	0.365	3.352	10.9
	EF-2/1	66	0.184	0.184	1.835	10.0
Wolfcamp	W-1/3	36	0.175	0.175	1.388	12.6
	W-2/1	22	0.106	0.106	1.147	9.2
Barnett	Br-1/1	59	0.170	0.170	0.730	23.3
	Br-2/3	42	0.254	0.254	1.630	15.6

In the same line, and contrary with oil imbibition results, Eagle Ford and Wolfcamp samples show much lower water imbibition as well as penetration magnitudes compared to oil. In the previous section, it is shown that oil imbibe Eagle Ford and Wolfcamp cores up to 76% of the pore volume whereas water only imbibe up to 20% in the best case with an average of 11%. These results are a clear indication that samples from Eagle Ford and Wolfcamp have higher affinity to oil than water, which is also confirmed by CA measurements. Nevertheless, the presence of organic and inorganic matter make water able to imbibe the cores but in lower quantities. Then, Barnett imbibition numbers also show slightly higher imbibition by water than oil coherent with CA measurements.

CT scan images from selected cores showing changes in densities related by CT numbers are illustrated in **Fig. 23**. All cores show a distinct increase in CT numbers before

pressures negative in sign suppressing water to efficiently imbibe the cores. Only core intermediate-wetness allows capillary pressure to be positive in sign and permits water to penetrate the rock and displace oil in countercurrent movement as evidenced in **Fig 26**.

Table 10. Spontaneous imbibition experiment results. Reprinted with permission from Alvarez and Schechter (2016c)

ULR	Well / Sample	Penetration magnitude (HU)	Δ Weight (gr)	N_b^{-1} (-)	Oil Recovered (% OOIP)
Bakken	Bk-1/1	9	0.09	938	7.8
	Bk-2/1	7	0.08	5516	4.1
Eagle Ford	EF-1/2	8	0.01	8452	2.8
	EF-1/4	7	0.02	9984	3.9
Wolfcamp	W-1/3	7	0.02	11095	3.5
	W-1/4	13	0.05	8611	5.1

As shown, imbibition is responsible of recovering oil in these ULR cores by replacing oil in the matrix by water. In order to assess further the type of forces that are contributing to water imbibition and corroborate the type of fluid movement, the inverse Bond number (Eq. 7) is used. This ratio of gravity to capillary forces determines which force is a dominant, gravitational force as cocurrent flow or capillary force as countercurrent flow. Table 9 shows high inverse Bond numbers for ULR cores from Bakken, Eagle Ford and Wolfcamp. In fact, all inverse Bond numbers are decidedly greater than 5, which confirms that capillarity is responsible of fluid movement and spontaneous imbibition of water into the rocks and fluid flow occurs counter currently, corroborating what was observed in Fig. 16. Capillarity is the main force driving oil production in these experiments because of the inverse effect of pore radius as stated in

these experiments serve as a screening process when several surfactants are tested. The results from this chapter are analyzed according to the capability of surfactants of altering wettability of the rock from its original state towards water-wet and reducing IFT without reaching ultralow values.

Surfactant Stability and Emulsion Tendency Test

Chemical additives stability tests were initially performed with seven different surfactants: two anionic, two nonionic and two blended (nonionic-cationic and nonionic-anionic) surfactants and a complex nanofluid (CNF). These chemical additives are currently offered and used by service companies in hydraulic fracture operations in the Permian Basin. For this study and based on stability test results, some of these surfactants were used in the subsequent experiments. The description of the surfactants used is in **Table 11**.

Table 11. Surfactant properties

Surfactant	Primary Components	Concentration (wt.%)	pH	Specific Gravity
Anionic A	Methyl alcohol	40-70	5.8-7.2	0.866 - 0.892
	Proprietary sulfonate	10-30		
Anionic B	Methyl alcohol	10-30	4.7-5.7	0.974 - 0.999
	Proprietary Sulfonate	7-13		
Nonionic A	Branched alcohol oxyalkylate	10-30	5.0-7.0	0.997 - 1.027
Nonionic B	2-Butoxyethanol	10-30	7.2-9.3	0.964 - 0.989
	Methyl alcohol	10-30		
	Petroleum naphtha	1-5		
Nonionic-Cationic	Ethoxylated isodecyl alcohol	10-30	7.0 - 9.0	1.016 - 1.046
	Quaternary ammonium compound	5-10		
	Quaternary ammonium compound	1-5		
Nonionic-Anionic	Methyl alcohol	60-90	6.3-7.3	0.823 - 0.848
	Proprietary ethoxylated alcohol	7-13		
	Proprietary sulfonate	5-10		
CNF	Isopropyl Alcohol	10-30	6.8-8.3	0.953 - 0.956
	Citrus Terpenes	10-30		
	Proprietary	10-20		

Surfactant solutions, during 10 days in an oven at reservoir temperature, were visually investigated to assess surfactant stability; the results after 10 days are shown in **Fig. 27 (top)**. From the seven surfactants tested, surfactants Anionic B and Nonionic B exhibited poor aqueous stability. In addition, emulsion tendency tests for the same surfactants and oil from the Wolfcamp are illustrated in **Fig. 27 (bottom)**.

Table 12. Lithological composition of rock samples from Wolfcamp wells W-1 and W-2

Well / Sample (Depth)	W-1 / 1 (7876 ft.)	W-1 / 2 (7880 ft.)	W-1 / 3 (7790 ft.)	W-2 / 1 (8370 ft.)
Mineral (wt. %)				
Quartz	42	41	13	48
Clays	26	27	16	27
Calcite	12	13	46	13
Dolomite	6	6	19	6
Feldspar	11	11	4	11
Pyrite	3	2	2	3
Relative Clay (%)				
Illite/mica	95.2	95.8	94.3	94.2
Smectite	4.8	4.2	5.7	5.8
Kaolinite	0	0	0	0
Chlorite	0	0	0	0

Dead crude oil from well W-1 had a black color with density of 0.82 g/cm^3 and 32.4° API at reservoir temperature of 165 °F. Moreover, using a Metrohm 905 Titrando apparatus, oil total acid number (TAN) and total base number (TBN) were determined. TAN and TBN values for Wolfcamp oil are 0.09 and 0.12 mg KOH/g oil, respectively. CA and zeta potential measurements for well W-2 were also performed using crude oil from well W-1, which is from the same area and reservoir.

Wolfcamp contact angle measurements results

The results for CA experiments for well W-1 at depths 1 and 2 (siliceous samples) described on Table 12, are shown in **Fig. 28** and **Fig. 29**. To have a baseline to compare wettability alterations and to address original wettability, CA measurements were performed with water without surfactants. The Frac Water bar represents the initial core

Wettability alteration results in the Eagle Ford formation

Core plugs and trims were received from the liquid rich portion of the Eagle Ford play. The samples were taken from well EF-1 at depths from 13,000 to 13,150 ft. and EF-2 at depths from 14,150 to 14,300 ft. Cores are 1-inch in diameter and 1.5 to 2.5-inches in length with porosities from 9 to 12 %, permeability to air of 100-300 nD, and median pore radii of 0.007 microns, all measured by MICP. Moreover, samples have total organic carbon (TOC) from 5.9 to 6.5 wt. %, measured on a LECO C230 Carbon Analyzer. XRD analysis for wells EF-1 and EF-2 at four different depths is provided in **Table 13** and shows carbonate as the predominant lithology present for the samples tested.

Table 13. Lithological composition of rock samples from wells EF-1 and EF-2

Well / Sample (Depth)	**EF-1 / 1 (13043 ft.)**	**EF-1 / 2 (13122 ft.)**	**EF-2 / 1 (14185 ft.)**	**EF-2 / 2 (14250 ft.)**
Mineral (wt.%)				
Calcite	60.2	53.9	58.5	53.9
Dolomite	0.9	1.1	0.0	1.0
Quartz	15.4	14.8	14.6	14.8
Clays	15.8	21.7	18.7	21.7
Pyrite	4.1	4.4	4.7	4.4
Plagioclase	2.6	3.0	2.7	3.0
Marcasite	1.0	1.1	0.0	1.1
Relative Clay (%)				
Illite/mica	60	59	60.3	54.2
Illite/Smectite	30	37	29.8	32.8
Kaolinite	3	1	2.3	4.5
Chlorite	7	3	7.6	8.5

Crude oil from well EF-2 is used with density of 0.72 g/cm^3 and 52.61° API at testing temperature of 180 °F. Oil total acid number (TAN) and total base number (TBN)

to 10,000 ft.) and Bk-2 (depths from 10,500 to 11,000 ft.). Mineralogical composition by XRD analyses from both wells at the studied depths are listed in **Table 14**. Lithology data indicates that well Bk-1 is mainly siliceous in composition whereas well Bk-2 is more carbonate. This information is vital to understand surfactant efficacy and wettability alteration mechanisms that are dependent on ULR mineral composition. In addition, Bakken dead crude oil is used with density of 0.7936 g/cm^3 and 37.30° API at 180 °F.

Table 14. Lithological composition of rock samples from wells Bk-1 and Bk-2

Well / Sample (Depth)	**Bk-1 / 1 (9620 ft.)**	**Bk-1 / 2 (9635 ft.)**	**Bk-2 / 1 (10765 ft.)**
Mineral (wt.%)			
Quartz	53	49	14
Clays	29	19	26
Calcite	3	26	0
Dolomite	4	3	51
Feldspar	9	2	9
Pyrite	2	1	0
Relative Clay (%)			
Illite/mica	69	67	60
Illite/Smectite	13	8	7
Kaolinite	4	9	11
Chlorite	14	16	22

Moreover, using a Metrohm 905 Titrando apparatus, oil total acid number (TAN) and total base number (TBN) were determined. TAN and TBN values for the Barnett oil are 0.36 and 0.23 mg KOH/g oil, respectively. CA and zeta potential measurements for wells Bk-2 were also performed using crude oil from well Bk-1 which is from the same area and reservoir.

porosities from 6 to 8 %, permeability to air of 750-1050 nD, and median pore radii of 0.007 microns, all measured by MICP. Moreover, samples have total organic carbon (TOC) from 1.7 to 2.5 wt. %, measured on a LECO C230 Carbon Analyzer. XRD analysis for wells Br-1 and Br-2 at three different depths is provided in **Table 15** and shows siliceous as the predominant lithology present for the samples tested.

Table 15. Lithological composition of rock samples from wells Br-1 and Br-2

Well / Sample (Depth)	**Br-1 / 1 (6060 ft.)**	**Br-1 / 2 (8018 ft.)**	**Br-2 / 1 (7030 ft.)**
Mineral (wt.%)			
Quartz	48	43	46
Clays	8	22	8
Calcite	35	18	38
Dolomite	6	7	6
Feldspar	2	8	1
Pyrite	1	2	1
Relative Clay (%)			
Illite/mica	91	90	76
Illite/Smectite	0	0	24
Kaolinite	11	5	0
Chlorite	0	5	0

Dead crude oils used were from the same wells as the cores with a viscosity of 30.0 cp and a density of 0.8080 g/cc at 165 °F and 37.74° API for Well Br-1, and 40.5 cp and a density of 0.8054 g/cc at 165 °F and 35.77° API for Well Br-2. Moreover, using a Metrohm 905 Titrando apparatus, oil total acid number (TAN) and total base number (TBN) were determined. TAN and TBN values for the Bakken oil are 0.27 and 0.55 mg KOH/g oil, respectively, for well Br-1, and 0.10 and 0.57 mg KOH/g oil, respectively, for well Br-2.

are also consistent with CA and zeta potential measurements where lithology impacted surfactant wettability alteration performance.

Surfactant adsorption results in the Eagle Ford formation

Adsorption measurements were performed in samples from Well EF-2 depth 1, as described in Table 13. Dynamic surfactant adsorption measurement results for surfactants anionic A and CNF, on sample EF-2/1 are shown on **Fig. 63**. As in the Bakken cores results, an increasing amount of surfactant adsorbed on the rock as time progresses, verifying the premise that the surfactant is adsorbed on the rock.

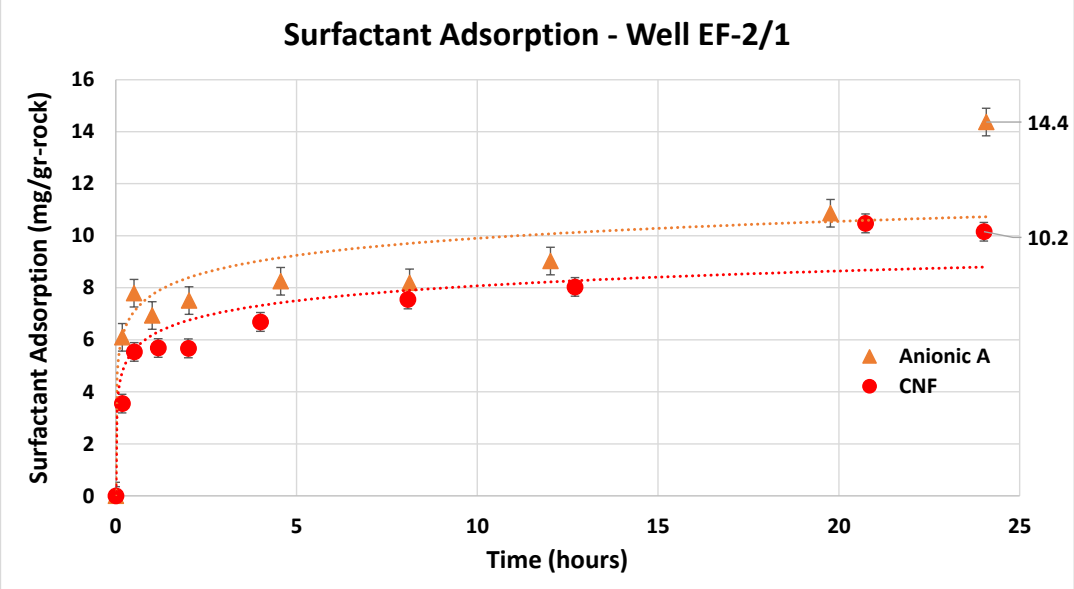

Figure 63. Surfactant adsorption measurement with time of well EF-2-1.

As shown in Table 13, the mineralogical composition of sample EF-2/1 is mainly carbonate with more than 58 wt.% calcite. When comparing the two surfactants on sample

After confirming a proof-of-concept regarding spontaneous imbibition in ULR, more detailed experiments were designed in other to capture changes in densities, fluid movements and imbibition as well as rates of recovery and ultimate recovery using modified Amott cells and CT scan technology.

Spontaneous Imbibition Experiments in the Wolfcamp Formation

Spontaneous imbibition experiments in ULR use siliceous cores from the Permian Basin. The experiments are conducted at reservoir temperature in an environmental chamber. All cores are from the same well, and they were aged in oil from the well at reservoir temperature (165 °F) for more than six months to reconstitute them with the missing liquid hydrocarbons due to sample handling. To confirm results repeatability, all experiments are performed twice on different cores from the same depth range. Moreover, aged unconventional siliceous and carbonate cores were submerged in aqueous solutions, with and without surfactants at reservoir temperature, to evaluate wettability changes, core fluid penetrations and the associated oil recoveries.

Initial core properties and type of fluid used for these experiments are shown in **Table 16**. These values were used to calculate original oil in place (OOIP) in cores. Moreover, porosities and initial water saturation (S_{wi}) value of 0.1 were provided by the core supplier and confirmed using mercury intrusion and extrusion analysis. To determine the initial wettability of the cores, CA measurements were performed on the samples.

Table 16. Initial core properties for Wolfcamp spontaneous imbibition experiments

Core	Diameter (in)	Length (in)	Porosity (%)	Initial CA (°)	Type of Fluid
1	0.980	1.59	6.4	139.2	Anionic A
2	0.979	1.48	6.4	131.4	Anionic A
3	0.982	1.70	6.5	139.8	Nonionic-Cationic
4	0.982	1.54	6.5	137.6	Nonionic-Cationic
5	0.973	1.78	6.5	139.1	Frac-Water
6	0.974	1.96	6.8	142.4	Anionic A
7	0.981	2.13	6.5	126.2	Anionic A
8	0.981	1.81	6.5	138.8	Nonionic-Cationic
9	0.984	2.04	6.5	135.6	Nonionic-Cationic
10	0.980	1.45	6.5	132.0	Frac-Water

At the beginning of the experiments, initial wettability measurement results showed cores with wettability of oil-wet towards intermediate-wet due to the extended aging period. Next, cores were submerged in different fluids as specified in Table 16. To address different surfactant types and their interactions with different rock lithologies, aqueous solutions of brine and surfactants anionic A and nonionic-cationic, at a concentration of 2 gpt, as well as brine alone were used. Regarding rock lithology, cores 1 to 5 were taken from Depth 1 and they were mostly siliceous with quartz as the predominant lithology (more than 40 wt.%), as shown in **Table 17**. Conversely, cores 6 to 10 were extracted from Depth 2 (Table 17) and there were predominately carbonate (more than 60 wt.%). Finally, to guarantee repeatability of our results, spontaneous imbibition experiments were performed twice with brine and surfactants on different cores and different lithologies from the same well.

Table 17. Lithological composition of rock samples from well W-1

Depth	**1 / (7876 ft.)**	**2 / (7790 ft.)**
Mineral (wt. %)		
Quartz	42	13
Clays	26	16
Calcite	12	46
Dolomite	6	19
Feldspar	11	4
Pyrite	3	2
Relative Clay (%)		
Illite/mica	95.2	94.3
Smectite	4.8	5.7

First, siliceous cores were evaluated, so cores 1 to 5 were submerged in aqueous solutions with and without surfactants as described in Table 16. The use of surfactant in spontaneous imbibition experiments accelerate oil recovery as shown in **Fig. 66**, for three of the five evaluated cores, in which oil was produced from core 1 (Anionic A) in less than 12 hours. Then, core 3 (Nonionic-cationic surfactant) began to expel oil at 36 hours. Lastly, core 5 (Frac water) began to produce oil at 48 hours. Similar behaviors were encountered for core 2 (Anionic A), core 4 (Nonionic-cationic surfactant). This faster oil production caused by imbibition in core 1 compared to cores 3 and 5 is explained by the fact that anionic surfactant changes wettability in the core faster due to its lower IFT which favors the imbibition of the aqueous phase into the core changing wettability faster, as showed in the IFT section of this manuscript. This change in wettability shifts capillary pressure from negative to positive mobilizing oil with the help also of gravity forces. In addition, because surfactant solution is imbibing into the core, its concentration is

applied to translate laboratory results to the field. Hence, we observed that imbibing fluids move throughout less resistance pathways inside the core, displacing hydrocarbon during the flow. Moreover, during the experiments, fluid countercurrent movement was evidenced where oil was expelled from the core surface as completion fluid imbibed due to changes in capillary pressure. Nevertheless, cores submerged in surfactant solutions showed visible changes in CT numbers indicating better imbibition compared to cores in frac-water, regardless of core lithology. This is consistent with oil recovery results (Fig. 67 and Fig. 68) and demonstrates that altering rock wettability and fluid IFT by the addition of surfactants improved the water penetration into the rock matrix, which consequently increased oil recovery.

Spontaneous imbibition experiment results are summarized in **Table 18** and **Table 19**. The cores used from Wolfcamp well WC-1 on the Permian Basin showed different penetration magnitude values, calculated using Eq. 29. For siliceous cores (cores 1-5), penetration magnitudes are seemingly higher for samples exposed to surfactant solutions than core submerged in water alone with the highest penetration by cores in surfactant anionic A. Similarly, carbonate cores (cores 6-10) showed higher imbibition by surfactant additives, but the highest penetration magnitude was evidenced by surfactant nonionic-cationic. These results qualitatively agree with oil recoveries by different surfactants and different lithologies, and corroborated our hypothesis that rock surface and surfactant charges play a vital role in imbibition and hydrocarbon production where electrostatic and hydrophilic rock-fluid interactions must be considered. Table 18 also shows changes in rock wettability, as determined by CA, before and after spontaneous imbibition

experiments. Cores in surfactant solutions changed their wettability from oil and intermediate-wet to water-wet; whereas cores submerged in frac-water without surfactant did not change the CA significantly enough to change wettability to water-wet.

Table 18. Wolfcamp spontaneous imbibition experiment results

Core	Type of Fluid	Initial Average CT (HU)	Final Average CT (HU)	Penetration magnitude (HU)	Final IFT (mN/m)	Initial CA (°)	Final CA (°)	Oil Recovery (%OOIP)
1	Anionic A	2066	2101	35	0.9	139.2	56.8	**33.9**
2	Anionic A	2214	2247	34	0.9	131.4	40.1	**28.5**
3	Nonionic -Cationic	2399	2425	26	7.4	139.8	59.4	**18.4**
4	Nonionic -Cationic	2253	2280	27	7.4	137.6	53.7	**19.7**
5	Frac-Water	2620	2632	12	22.1	139.1	111.9	**10.5**
6	Anionic A	2203	2225	22	0.9	142.4	46.4	**15.0**
7	Anionic A	2208	2226	19	0.9	126.2	56.0	**11.7**
8	Nonionic -Cationic	2231	2262	30	7.4	138.8	51.9	**24.5**
9	Nonionic -Cationic	2245	2273	27	7.4	135.6	55.1	**18.5**
10	Frac-Water	2218	2231	13	22.1	132.0	110.7	**7.1**

The ability of surfactant to alter wettability along with reducing IFT made possible for capillary pressure to shift from negative to positive values as shown in Table 1 and calculated by using Eq. 1. These changes in capillary forces for cores in contact with surfactants favored imbibition and improved oil recovery as demonstrated in the last column of Table 19. On the other hand, cores in frac-water without surfactants were not able to change capillary pressure sign and consequently did not favor imbibition marginally recovering oil only by the aid of fluid densities difference as gravity forces.

Table 19. Wolfcamp capillary pressure and inverse Bond numbers

Core	Type of Fluid	Initial Pc (psi)	Final Pc (psi)	N_b^{-1} (-)	Oil Recovery (%OOIP)
1	Anionic A	-1213	36	438	**33.9**
2	Anionic A	-1060	50	438	**28.5**
3	Nonionic-Cationic	-1224	273	3629	**18.4**
4	Nonionic-Cationic	-1183	318	3629	**19.7**
5	Frac-Water	-1211	-598	10838	**10.5**
6	Anionic A	-1270	45	594	**15.0**
7	Anionic A	-1206	36	581	**11.7**
8	Nonionic-Cationic	-947	331	4774	**24.5**
9	Nonionic-Cationic	-1145	307	4774	**18.5**
10	Frac-Water	-1072	-567	14258	**7.1**

In order to assess the impact of capillary forces with respect to gravity forces in these liquid rich shales from the Permian Basin, the inverse Bond number (Eq. 7) was calculated. The inverse Bond number represents the ratio of capillary forces to gravitational forces and determines when capillary forces drive imbibition as countercurrent flow or when gravitational forces drive it as cocurrent flow. From Schechter, Zhou, and Orr Jr (1994), I learned that when the inverse Bond number is greater than 5, capillary forces are responsible of imbibition. As shown in Table 19, inverse Bond numbers for these unconventional reservoirs with ultralow permeability were clearly greater than 5, which confirmed that capillary forces are the main driving force for aqueous solution imbibition. This observation is corroborated the by penetration magnitude and oil recovery exhibited in cores that changed wettability and reduced IFT using surfactants in contrast to cores in frac-water only.

wettability further was the one that recovered more oil, which leads us to conclude that rock-fluid interactions controlled imbibition and fluid flow. Hence, rock lithology and oil type should be considered and studied to select the proper surfactant additive for completion fluids to maximize oil recovery after stimulation.

Spontaneous Imbibition Experiments in the Eagle Ford Formation

This section presents the spontaneous imbibition results for brine with and without surfactant additives, which include wettability changes, penetration of the fluids into cores and the associated oil recovery. Initial properties of the samples used for these experiments are provided in **Table 20**. Core measurements as well as porosity and initial water saturation (S_{wi}) were used to calculate the OOIP. Porosities, shown in Table 20, and water initial saturations were provided by the core supplier and confirmed using mercury intrusion and extrusion analysis. For this study, initial water saturation used for the calculations was 0.15. Finally, core initial wettability was determined by CA methods as described in previous sections. The results in Table 4 show mostly intermediate towards oil-wet cores.

Table 20. Initial core properties for Eagle Ford spontaneous imbibition experiments

Core	Diameter (in)	Length (in)	Porosity (%)	Initial CA (°)	Type of Fluid
1	0.997	2.288	12.2	104.9	Frac-Water
2	0.999	1.165	12.0	123.2	Frac-Water
3	0.991	2.253	12.2	103.0	Anionic A (A)
4	0.998	1.453	12.0	132.5	Anionic A (A)
5	0.993	2.028	12.2	110.4	Nonionic-Cationic (NC)
6	0.995	1.643	12.0	120.2	Nonionic-Cationic (NC)
7	1.001	2.214	12.2	103.4	Complex Nanofluid (C1)
8	0.995	2.071	12.0	106.1	Complex Nanofluid (C1)
9	0.955	2.070	13.1	100.1	Anionic-Nonionic (AN)
10	0.994	1.953	13.1	96.0	Nonionic-Anionic (NA)
11	0.991	1.819	13.1	98.4	Complex Nanofluid 2 (C2)

Eagle Ford cores from well EF-2 were aged for more than 4 months at reservoir temperature and spontaneous imbibition experiments were conducted at 180 °F. In addition, XRD analysis shows that all cores used have carbonate as the predominant lithology (more than 60 wt.% carbonates). The same surfactants tested in CA, zeta potential and IFT experiments, described in Table 11, Chapter 5, were used at a concentration of 2 gpt. In addition, I added two more surfactants to the set of spontaneous imbibition experiments, their description is in **Table 21**, and the other surfactant properties are in Table 11, Chapter 5.

Table 21. Surfactant properties 2

Surfactant	Primary components	Composition (wt.%)	pH	Specific Gravity
Anionic + Nonionic **(AN)**	Methyl alcohol	10-30	4.7 - 5.7	0.97 - 0.99
	Proprietary Sulfonate	7-13		
Complex Nanofluid 2 **(C2)**	Isopropyl alcohol	5-40	5.0 - 8.0	0.96 - 1.01
	Citrus Terpenes	5-15		

Moreover, to guarantee repeatability of our results, experiments with brine and surfactants Anionic A (A), Nonionic-cationic (NC) and CNF (C1) were performed twice on different cores from the same well. To that end, cores 1 and 2 were tested with frac-water, cores 3-4 with anionic surfactant (A), cores 5-6 with nonionic-cationic surfactant (NC), cores 7-8 with CNF (C1), core 9 with surfactant anionic-nonionic (AN), core 10 with surfactant nonionic-anionic (NA) and core 11 with complex nanofluid 2 (C2).

The oil expelled by imbibition from the cores was measured using a graduated cylinder at the top of the modified Amott cells. **Fig. 71** shows oil recovery, as function of the OOIP, with time. After rigorously follow the development of the experiments, we identified three marked stages for oil recovery as shown in Fig. 71. The very first stage (stage 1) shows greater recovery rates in the first 12 hours. In addition, the cores submerged in surfactant solutions begin to produce oil faster that brine alone. These observations are explained by the capability of surfactants of reducing IFT. During early time of the experiments, capillary pressures were still negative because wettability alteration has not taken place yet. However, IFT reduction on aqueous solution-oil

wettability alteration potential. Moreover, penetration magnitude values correlated with oil recovery reinforcing the relation of imbibition and hydrocarbon production in these ultralow permeability cores.

Table 22. Eagle Ford spontaneous imbibition experiment results

Core	Type of Fluid	Initial Average CT (HU)	Final Average CT (HU)	Penetration magnitude (HU)	IFT (mN/m)	Initial CA (°)	Final CA (°)	Oil Recovered (% OOIP)
1	Frac-water	1847	1855	8	34.03	104.9	94.7	**1.9**
2	Frac-water	1816	1822	7	34.03	113.2	93.2	**2.9**
3	A	1865	1881	17	0.22	103.0	35.8	**6.8**
4	A	1771	1787	16	0.22	132.5	40.3	**6.6**
5	NC	1852	1871	19	1.76	110.4	39.9	**9.3**
6	NC	1765	1782	18	1.76	120.2	36.4	**10.0**
7	C1	1842	1857	15	2.33	103.4	34.3	**6.6**
8	C1	1776	1792	16	2.33	106.1	46.4	**7.6**
9	AN	1827	1840	13	2.89	100.1	39.2	**3.6**
10	NA	1840	1857	17	4.48	96.0	41.2	**4.6**
11	C2	1834	1845	11	7.25	98.4	77.5	**3.1**

Initial CA confirmed the presence of intermediate towards oil-wet core Final CA and IFT showed the capability of surfactant additives to alter wettability to water-wet and reduce oil-water IFT. In addition, final CA suggested that solution without surfactant additives were not able to alter wettability or reduce IFT, which had a direct impact in on capillary pressure. As showed, initially capillary pressures are negative for all cores due to initial wettability states. As the experiments progress and surfactant solutions alter wettability, capillary forces turned positive favoring imbibition and consequently oil recovery as demonstrated on the last column of Table 23. On the other hand, capillary

pressures for cores in frac-water still showed negative values at the end of the experiments, this is the main reason for low penetration and hydrocarbon production.

Table 23. Eagle Ford capillary pressures and inverse Bond numbers

Core	Type of Fluid	Initial Pc (psi)	Final Pc (psi)	Oil Recovered (% OOIP)
1	Frac-water	-363	-116	1.9
2	Frac-water	-556	-79	2.9
3	A	-317	7	6.8
4	A	-953	7	6.6
5	NC	-492	56	9.3
6	NC	-709	59	10.0
7	C1	-327	80	6.6
8	C1	-391	67	7.6
9	AN	-247	93	3.6
10	NA	-147	140	4.6
11	C2	-206	65	3.1

In summary, the results of these correlated set of experiments show that wettability alteration and IFT reduction play a significant role on improving the penetration of stimulation fluid into the rock matrix, which also improve oil recovery. Rock wettability must be shifted from intermediate and oil-wet to water-wet to let capillary forces promote imbibition and release trapped hydrocarbons. In addition, moderate IFT reductions are needed to trigger wettability alteration by pore imbibition. However, contrary to conventional EOR in which IFT is required to be reduced to almost zero, in liquid rich shales, IFT should not be greatly reduced to avoid oil redeposition into the pores and eliminate capillary forces as a driving mechanism. Moreover, rock surface charges as well

as oil and surfactant impact imbibition and oil recovery, thereby they must be considered when choosing the best suitable treatment for the reservoir.

Spontaneous Imbibition Experiments in the Bakken Formation

In Chapter V, I corroborated that adding chemical additives like surfactants and CNF to completion fluids alters wettability of Bakken cores from oil-wet to water-wet and reduces water-oil IFT. These changes in CA and IFT modify capillary pressure to favor spontaneous imbibition. Bakken cores from wells Bk-1 (predominately siliceous) and Bk-2 (predominately carbonate) were aged in Bakken oil for more than 6 months at reservoir temperature to reconstitute them with the missing liquid hydrocarbons due to sample handling. Moreover, spontaneous imbibition experiments were performed in an environmental chamber at 180 °F. For both wells, core dimensions, initial properties, and type of fluid used are in **Table 24**. These values are used to calculate the original oil in place (OOIP) and obtain oil recovery with times as experiments progress. Bakken initial water saturation (S_{wi}) for well Bk-1 is 0.38 and for well Bk-2 is 0.20; we used these values to calculate OOIP. In addition, core initial wetting affinity is measured by CA methods. Table 24 shows that all cores are initially oil-wet due to the extended aging period.

Table 24. Initial core properties for Bakken spontaneous imbibition experiments

Core	Well	Porosity (%)	OOIP (cm^3)	Initial CA (°)	Type of Fluid
1	Bk-1	10.8	1.672	121.0	Water
2	Bk-1	10.8	1.780	120.6	Anionic A
3	Bk-1	10.8	1.797	122.6	Nonionic-cationic
4	Bk-1	10.8	2.183	117.2	CNF
5	Bk-2	6.5	0.945	121.7	Water
6	Bk-2	6.5	0.985	126.7	Anionic A
7	Bk-2	6.5	1.022	120.5	Nonionic-cationic
8	Bk-2	6.5	0.816	119.1	CNF

The first set of experiments is performed with cores from well Bk-1. Cores 1 to 4 are submerged in aqueous solutions with and without surfactants and CNF as specified on Table 24. The concentration used for surfactant and CNF was 2 gpt. Using the graduated cylinder at the top of the modified Amott cells, oil production for all experiments is recorded with time and reported as function of the OOIP. This is shown in **Fig. 73** where surfactant Anionic A performed better than CNF and surfactant Nonionic-cationic, and all solutions with chemical additives recover more oil than water alone, which is consistent with CA, zeta potential, and IFT results. Surfactant Anionic A produces more oil from these Bakken siliceous cores because it alters wettability in higher amounts and reduces IFT to lower values. Lower IFT favors water penetration in the nanopores, changing wettability by electrostatic interactions. I suggest that Anionic surfactant heads form ion-pairs with the oil in the pores and strip it from the rock surface. Then, by imbibition, water replaces the oil in-situ, expelling it out of the cores in a countercurrent movement. In the process, capillary pressure not only changes from negative to positive, but also its value is reduced due to IFT alteration. This mobilizes liquid hydrocarbons from the ULR cores

fractures are created favoring water imbibition and oil expulsion from the matrix. Even though water imbibition may not seem uniform along the cores due to rock heterogeneities, an imbibition profile is observed in our experiments, as positive changes in CT numbers, and more importantly, oil is recovered in higher amounts when using surfactants and CNF additives. Thus, CT scan methods provide reliable means to oversee completion fluid imbibition in Bakken cores, which can be related to hydrocarbon production (Alvarez, Saputra, and Schechter 2017).

The aqueous solution imbibition or penetration magnitude in the cores related by Eq. 29 is shown in **Table 25**. The differences between initial and final core average CT numbers can tell us comparatively the amount of fluid that imbibes in each experiment. The results for well Bk-1 show that core 1 (water alone) has the lowest penetration magnitude whereas cores 2-4, surfactant Anionic A, Nonionic-cationic, and CNF, respectively, have higher values compared to core 1. In fact, core 2 is shows the highest penetration magnitude followed by cores 4 and 3. These results are consistent with oil recovery for well Bk-1 cores. In addition, Table 25 also point out initial and final core weights. Due to water imbibition and oil expulsion, cores are expected to weigh more at the end of the experiments. This is the case for all the cores in well Bk-1; however, cores 2 to 4 have higher changes in weight as an indication of better imbibition, while core 1 has a much lower value due to its limited water imbibition.

Table 25. Bakken spontaneous imbibition experiment results

Core	Type of Fluid	Initial Average Core CT (HU)	Final Average Core CT (HU)	Penetration magnitude (HU)	Initial Weight (gr)	Final Weight (gr)	Initial CA (°)	Final CA (°)
1	Water	1761	1770	9	62.784	62.881	121.0	99.9
2	Anionic A	1762	1789	27	66.695	66.859	120.6	44.5
3	Nonionic -cationic	1760	1782	22	67.351	67.475	122.6	55.1
4	CNF	1767	1791	24	81.370	81.530	117.2	46.1
5	Water	1954	1961	7	46.043	46.126	121.7	109
6	Anionic A	1950	1969	19	49.600	49.727	126.7	49.6
7	Nonionic -cationic	1952	1973	21	51.228	51.349	120.5	51.0
8	CNF	1956	1981	25	40.670	40.808	119.1	43.8

Similarly, to penetration magnitudes for well Bk-1, changes in weight are consistent with oil recoveries. Finally, for well Bk-1, initial and final CA as values for wetting affinity are shown in Table 25. As explained before, all well Bk-1 cores are initially oil-wet, but after the spontaneous experiments cores 2 to 4 change their wettability to water-wet due to the interaction with surfactants and CNF as shown in **Fig. 77**. On the other hand, core 1 barely changes CA towards intermediate-wet, but it does not reach the water-wet behavior (Fig. 77). The lack of wettability changes in core 1 is the reason why penetration magnitude is the lowest as well as the change in weight; therefore, water imbibition is limited and oil recovery is the lowest among the cores evaluated.

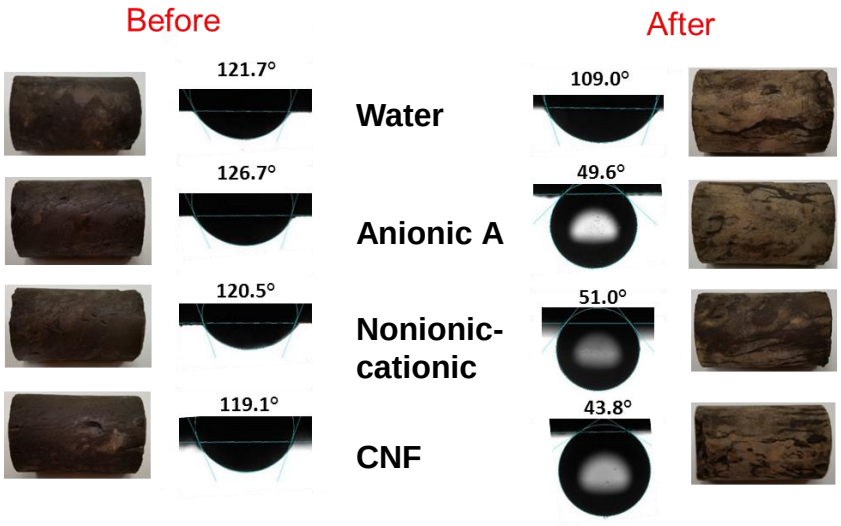

Figure 78. Contact angles before and after spontaneous imbibition experiments for well Bk-2 cores.

The results for both wells show water imbibition by penetration magnitude and wettability changes by CA measurements. These alterations along with changes in IFT are responsible for better oil recovery for the cores in contact to aqueous solutions with surfactants and CNF. To that end, capillary pressures (Eq. 1), before and after the experiments, are calculated using CA, IFT, and pore radius (Table 6) for each core and shown in **Table 26**. For all cores, initial capillary pressures are negative with high values, especially for cores from well Bk-2 with smaller pore radius. Pore radius inversely affects capillary pressure; so, the smaller the pores, the higher the capillary pressure and the more difficult it is to displace oil by imbibition. In fact, in oil-wet systems, spontaneous imbibition does not take place because oil is captured by the matrix, driven by capillarity. When wettability and IFT are altered by addition of surfactants and CNF, capillary pressure not only changes from negative to positive, but also reduces its value low enough

to let the aqueous solution invade the cores and drive oil out in countercurrent movement. Conversely, the lack of alteration in wettability and IFT in the cores 1 and 5 is responsible for their lower oil recovery as compared to the other cores (Alvarez and Schechter 2016a).

Table 26. Bakken capillary pressure and inverse Bond numbers

Well	Type of Fluid	IFT (mN/m)	Initial Pc (psi)	Final Pc (psi)	N_b^{-1} (-)	Oil Recovered (% OOIP)
Bk-1	Water	17.2	-76	-25	938	**15.9**
Bk-1	Anionic A	0.3	-75	2	16	**40.6**
Bk-1	Nonionic-cationic	4.5	-79	22	245	**31.3**
Bk-1	CNF	1.5	-67	9	85	**36.8**
Bk-2	Water	17.2	-262	-162	5513	**8.4**
Bk-2	Anionic A	0.3	-298	6	96	**23.6**
Bk-2	Nonionic-cationic	4.5	-253	82	1444	**27.8**
Bk-2	CNF	1.5	-243	31	481	**33.9**

In addition to capillary pressure, the inverse Bond number (Eq. 7) was calculated to address the ratio of capillary to gravitational forces and to determine if imbibition is driven by gravitational forces as cocurrent flow or driven by capillary forces as countercurrent flow. As shown in Table 26, inverse Bond numbers are significantly higher than 5, which corroborates that the main force propelling spontaneous imbibition in these Bakken cores is capillarity favoring countercurrent flow. In general, due to their ultra-low permeability, ULR have high inverse Bond numbers, which implies that capillary forces are more important than gravitational forces in controlling imbibition.

In summary, for wells Bk-1 and Bk-2, surfactants and CNF clearly show better performance over water alone in altering wettability, as determined by CA and zeta

Three different types of surfactants were used, as described in Table 11 and complemented in **Table 27:** anionic A, nonionic-cationic, and complex nanofluid 3 (CNF-3). These surfactants, as well as slickwater without surfactants, were tested to address their effectiveness in penetration into the fractures and recovering oil from ULR cores. These solutions were injected through the fractures at reservoir conditions. Then, a soak and produce scheme was used to simulate fracture-treatment and flowback. Initial and final core wettability were determined by contact angle. Changes in IFT were measured by the pendant drop method.

Table 27. Surfactant properties 3

Surfactant	Primary components	Composition (wt.%)	pH	Specific Gravity
Complex Nanofluid 3 **(CNF-3)**	Isopropyl alcohol	7-13	6.41	1.00-1.06
	Citrus Terpenes	10-30		
	Sulfonated surfactant	10-30		

Core Flooding Imbibition Experiments Results in ULR

Liquid rich shale cores from the Wolfcamp ULR were used. Sidewall cores had a diameter of 1-inch and a length of 1.5 to 3-inches. All cores were from well W-2, as described in Table 3. TOC content ranged from 4.5 to 5.7 wt.%, which was measured on a LECO C230 Carbon Analyzer. In addition, X-Ray Diffraction (XRD) analysis for the cores used describes core mineralogy as shown in **Table 28**. Samples depths range from

8390 to 8405 ft., and they are predominately carbonaceous with calcite and dolomite contents of more than 50 wt.%.

Table 28. Lithological composition of rock samples from well WC-2

Sample / Depth (ft)	**1 / (8405)**	**2 / (8400)**	**3 / (8395)**	**4 / (8390)**
Mineral (wt. %)				
Quartz	22	20	24	22
Clays	20	23	20	22
Calcite	36	36	30	32
Dolomite	16	15	19	17
Feldspar	5	4	4	5
Pyrite	1	2	3	2
Relative Clay (%)				
Illite/mica	96.2	96.0	95.5	95.1
Smectite	3.8	4.0	4.5	4.9

Petrophysical analyses, measured by mercury injection capillary pressure (MICP), showed permeability to air from 100 to 200 nD for the carbonate cores, with both having core porosities ranging from 6 to 7%, and median pore radius of 0.005 microns.

Initial core properties and type of fluid used for these experiments are shown in **Table 29**. These values were used to calculate original oil in place (OOIP) in cores. Moreover, initial oil saturation (S_{oi}) value of 0.65 was provided by the core supplier and confirmed using mercury intrusion and extrusion analysis. To determine the initial wettability of the cores, CA measurements were performed on the samples.

Table 29. Initial core properties for Wolfcamp core flooding imbibition experiments

Core	Diameter (in)	Length (in)	Porosity (%)	Initial Weight (gr)	Initial CA (°)	Type of Fluid
1	0.987	2.995	6.3	95.39	131.2	Anionic A
2	0.986	3.465	6.4	105.16	141.0	Nonionic-Cationic
3	0.987	3.587	6.4	110.06	133.6	CNF-3
4	0.986	3.436	6.4	107.99	130.3	Frac-water

Initial wettability measurement results showed cores with wetting affinity of oil-wet to intermediate-wet due to the extended aging period. Then, core-flooding imbibition experiments were performed by varying the type of fluid injected. Due to core ultralow permeability, fluid flow was expected to occur throughout the fractures. However, wettability and IFT alterations induced by surfactants would trigger imbibition on the fractures towards the matrix, improving oil recovery compared to a system injecting slickwater alone. The first part of the experiment aims to reproduce the soaking stage that a well undergoes when a completion fluid is left on the propped fractures for an extended period. To accomplish this, aqueous solutions containing different surfactants at concentration of 2 gpt as well as slick water alone were injected at reservoir conditions of 165 °F and 1500 psi and soaked into the core-flooding system for 72 hours. During the soaking period, CT scan images were taken to assess the penetration magnitude or imbibition of completion fluids inside the core. **Fig. 79** shows the behavior of average change of CT number, or penetration magnitude (Eq. 29), with time in cores 1 to 4. As used in spontaneous imbibition experiments, KI was added as a dopant to better

hydrophobic interactions, while the oil layer attached to the shale surface forms a double layer with the hydrophobic surfactant tails. Thereby, the hydrophilic surfactant heads face the aqueous solution, altering wettability and creating a water-wet zone.

Table 30 summarizes the experimental results for the four core flooding experiments. Penetration magnitudes compare the amount of fluid that imbibes in each experiment. The results show that core 4 (frac-water) has the lowest penetration magnitude whereas cores 1-3, surfactant Anionic A, nonionic-cationic, and CNF-3, respectively, have higher values compared to the magnitude of core 4. Also, core 2 shows the highest penetration magnitude followed by cores 1 and 3. These results are consistent with final oil recovery. In addition, Table 30 also shows the cores change in weight. Cores are expected to weigh more at the end of the experiments because imbibition replaces a lighter fluid (oil) by a heavier fluid (water), so the change should be positive in magnitude. This is the case for all the cores tested. Moreover, cores 1 to 3 display higher changes in weight as an indication of larger imbibition, while core 4 has a much lower value confirming its limited water imbibition. Consistent to the obtained penetration magnitudes results, changes in weight also show correlation with oil recoveries.

Table 30. Core flooding imbibition experiment results

Core	Type of Fluid	Penetration magnitude (HU)	Δ Weight (gr)	Δ CA (°)	Δ IFT (mN/m)	Initial Pc (psi)	Final Pc (psi)	Oil Recovered (% OOIP)
1	Anionic A	23	0.14	75.2	20.9	-845	29	**7.2**
2	Nonionic cationic	32	0.32	91.2	14.4	-996	281	**13.3**
3	CNF-3	20	0.19	78.5	17.6	-884	139	**6.9**
4	Frac-water	12	0.09	37	0	-829	-73	**2.0**

In addition, changes in CA are also shown in Table 30. Core flooded with nonionic-cationic surfactant (core 2) has the highest change in contact angle, followed by cores 3 and 1 (CNF-3 and anionic A). Conversely, core 4 barely changed the CA, not reaching water-wetness and, consequently, not promoting water imbibition into the core. Changes in IFT are also in Table 30. Surfactant anionic A shows the highest variation among all surfactants tested, followed by CNF-3 and nonionic-cationic surfactants. Wettability alteration results correlates with oil recovery, whereas IFT changes does not correlate. The results indicate that wettability alteration dominates imbibition over IFT reduction in theses ULR. Nevertheless, surfactant capability of moderately reducing IFT is vital to capillary forces reduction and wettability alteration. Surfactants reduce IFT low enough to reduce capillary pressures and let fluids imbibe into the pores and alter wettability by cleaning or coating the rock surface.

Finally, using the Young-Laplace equation (Eq. 1), we calculated capillary pressures. Initially, due to oil-wetness and small pore radius, capillary pressures are negative with large values. Wettability gave the negative sign and pore radius gave the large magnitude value. In fact, in ULR, capillary forces are elevated because the small pore sizes impact oil displacement by imbibition. Then, as wettability is altered and IFT moderately reduced by surfactants (cores 1 to 3), capillary pressures change sign from negative to positive and reduce their magnitude low enough to let the aqueous solutions invade the matrix from the fractures and expel oil out to the fractures in a countercurrent movement. Contrarily, frac-water alone (core 4) is not capable of altering either

on the field. As shown in Fig. 71, stage 1 exhibits larger production rates in the first 12 hours as surfactant solution penetrates the core surface due to a decrease in IFT. At stage 2 (after 12 hours), wettability alteration takes place and production rates are relatively stable because capillary pressure sign changed and remained nearly constant. By stage 3 (after 70 hours), the production rates decreased to almost zero due to the size of core samples.

Upscaling data from the laboratory to the field was done using the experimental data from cores 2, 4, 6, and 8. We chose these cores to compare the impact of production profiles by using different surfactant types and slickwater alone. For spontaneous imbibition experiments, the average end time of high production was 10 hours. Using core dimensions in Table 20, the characteristic lengths of core samples were calculated using Eq. 30 and shown in **Table 31**. In addition, field characteristic lengths were calculated using Eq. 31.

Table 31. Characteristic core lengths for the Eagle Ford

Core	Type of Fluid	$L_{c(Lab)}$ (cm)	$L_{c(field)}$ (cm)
2	Frac-water	0.767	79.722
4	A	0.806	83.780
6	NC	0.821	85.362
8	C1	0.846	87.924

For the scaling process, we assumed that the induced fractures form one layer of equal-sized cube matrix blocks along both sides of the hydraulic fracture as shown in **Fig. 89.** We also assumed that the imbibition process only happens in the opened blocks. Field scale spontaneous imbibition can be equivalent to spontaneous imbibition for these cube

Table 32. Completion methods and fracture geometries

Case	Number of Stages	Number of HF per stage	HF Half-length (ft.)
1	15	2	200
2	15	4	200
3	15	4	400
4	30	4	400

After carefully analyzing field production data from the same Eagle Ford area as the samples tested, we observed that the production rate decreased to less than 30% of maximum production after one year and then to a very low value after five years of production. Thereby, we decided to predict five years of production rates for all cases. **Fig. 90** shows the field production rate curves for all cases.

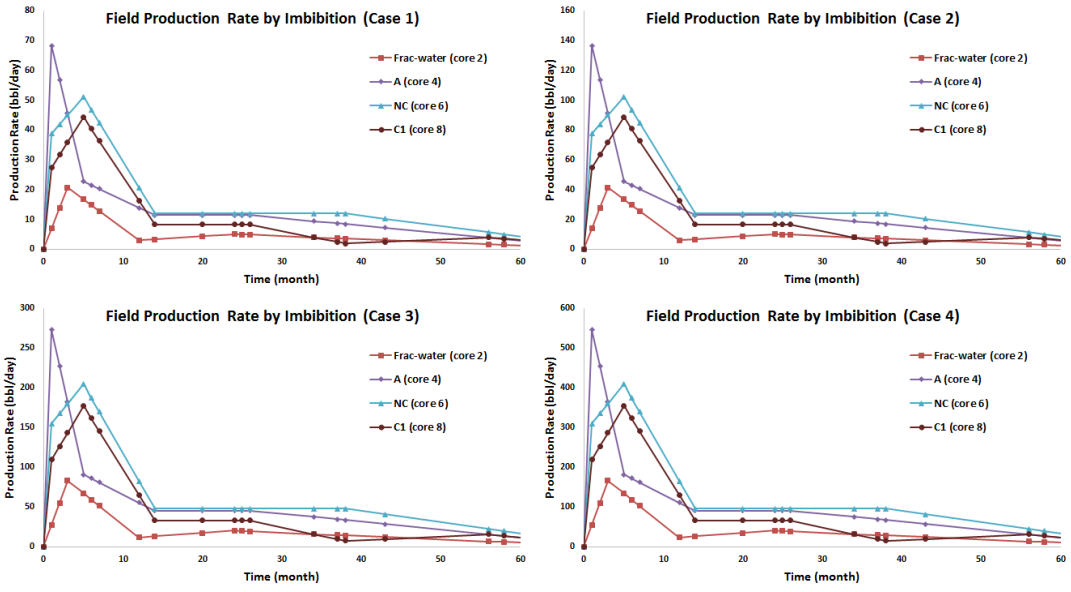

Figure 90. Predicted field production rates by imbibition from scaling laboratory data in the Eagle Ford.

Upscaled field production data shows that surfactant Anionic A has the highest peak, and its production rate decreased rapidly. The high initial production is due to the capability of surfactant Anionic A in reducing IFT. Then, surfactant NC dominates imbibition because its capability in altering wettability largely than surfactants with anionic compounds. Lastly, all cores submerged in surfactant solutions showed higher field production rates than the production rates from cores in slickwater alone.

Moreover, as fracture geometries increased from case 1 to 4, production rates also increase. Production rates driven by imbibition show the impact of surfactants in oil recovery. In fact, imbibition aided by surfactants increased oil production rate by 50 bbl/day in case 1 to almost to 375 bbl/day in case 4. These findings highlight the importance of imbibition and corroborate that fracture density and rock-fluid interactions are key parameters for oil recovery in these ULR. The results showed that the close presence of induced fractures to the hydraulic fracture results in economic production rates, and the use of surfactants could effectively improve oil recovery in fractured ULR.

Cumulative field oil production dominated by imbibition was calculated using Eq. 33 and listed for all cases in **Table 33**. Surfactant NC (core 6) achieved the highest cumulative oil production for all four cases, which matched the experiments results. As total opened fracture area increased (from case 1 to case 4), the predicted oil accumulation for imbibition also increased. This rising trend in oil production as fracture density increases is due to the improved oil recovery by imbibition because of a higher area of contact with the rock surface by the aqueous solutions.

Table 33. Cumulative field oil production by imbibition for the Eagle Ford

		Cumulative Oil Production (bbl)			
Core	**Type of Fluid**	**Case 1**	**Case 2**	**Case 3**	**Case 4**
2	Frac-water	6,614	13,228	26,455	52,910
4	A	16,400	32,800	65,600	131,200
6	NC	24,530	49,059	98,119	196,237
8	C1	19,141	38,282	76,563	153,127

Until now, the upscaling results obtained correspond to the amount of oil that would be recovered by altering wettability and IFT to favor imbibition of completion fluids in a soaking and flowback completion scheme. However, the oil produced by pressure differences between the reservoirs and wellbore also contributes significantly to total oil production. Hence, total well-oil production is the contribution of both fluid flow driven by pressure difference and imbibition. We used real-field production data, retrieved from IHS Energy database, of the wells from the same county as core sample as a base case for the pressure difference contribution. Therefore, as shown in **Fig. 91**, production rates are the sum of the actual field production data and the oil recovered by imbibition in each case.

their maximums. These production rate curves are like actual production rate curves observed on the field.

Upscaling data from the laboratory to the field was done using the experimental data to compare the production profiles by using different surfactant types and frac-water alone. Using core dimensions in Table 16 (cores 1 to 5), the characteristic lengths of core samples were calculated with Eq. 30 and shown in **Table 34**. In addition, field characteristic lengths were calculated using Eq. 31.

Table 34. Characteristic core lengths for Wolfcamp

Core	Type of Fluid	$L_{c(Lab)}$ (cm)	$L_{c(field)}$ (cm)
1	Anionic A	0.807	45.936
2	Anionic A	0.796	45.335
3	Nonionic-cationic	0.816	46.477
4	Nonionic-cationic	0.803	45.740
5	Frac-water	0.794	45.204

Similar as the scaling process for the Eagle Ford, we assumed that the induced fractures form one layer of equal-sized cube matrix blocks along both sides of hydraulic fracture, and assume that the imbibition process only happens in the opened blocks. Field scale spontaneous imbibition can be equivalent to spontaneous imbibition for these cube matrix blocks surrounded by aqueous solution. Hence, the side length of these matrix blocks can be obtained based on $L_{c(field)}$, which is used to determine the total well-oil production by spontaneous imbibition. In the same way, we tested the same four completion scenarios and hydraulic fracture geometries as that in the Eagle Ford section, and shown in Table 22. Finally, the prediction time was limited to five years because after

consistent with the laboratory results explained in Chapter VII, and stressing the impact of wettability and IFT alteration in imbibition and oil recovery. This better performance of surfactant Anionic A is due to its efficacy in altering wettability and reducing IFT better than the nonionic-cationic surfactant. Nevertheless, all cores submerged in surfactant solutions show higher field production rates than the cores in frac-water alone, confirming the role of surfactants in imbibition.

Next, cumulative field oil production dominated by imbibition was calculated using Eq. 33 and listed for all cases in **Table 35**. Surfactant Anionic A (cores 1 and 2) achieved the highest cumulative oil production for all four cases followed surfactant nonionic-cationic surfactant (core 3 and 4). These results match the experiments results obtained in Chapter VII. In addition, as total opened fracture area increased (from case 1 to case 4), the predicted oil accumulation for imbibition also increased, confirming the impact of fracture density on oil recovery.

Table 35. Cumulative field oil production by imbibition for the Wolfcamp

		Cumulative Oil Production (bbl)			
Core	**Type of Fluid**	**Case 1**	**Case 2**	**Case 3**	**Case 4**
1	Anionic A	25,190	50,381	10,0761	20,1522
2	Anionic A	20,879	41,759	83,518	167,036
3	Nonionic-cationic	13,576	27,152	54,303	108,607
4	Nonionic-cationic	14,804	29,609	59,217	118,434
5	Frac-water	5,302	10,603	21,206	42,412